Heat generation mechanisms of DBD plasma actuators

RODRIGUES, Fredrico <http://orcid.org/0000-0001-8904-607X>, PASCOA, Jose <http://orcid.org/0000-0001-7019-3766> and TRANCOSSI, Michele <http://orcid.org/0000-0002-7916-6278>

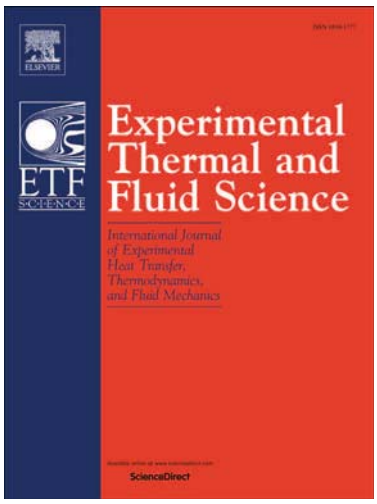

Heat Generation Mechanisms of DBD Plasma Actuators

F. Rodrigues, J. Pascoa, M. Trancossi

PII: S0894-1777(17)30269-8
DOI: http://dx.doi.org/10.1016/j.expthermflusci.2017.09.005
Reference: ETF 9205

To appear in: *Experimental Thermal and Fluid Science*

Received Date: 15 May 2017
Revised Date: 26 July 2017
Accepted Date: 5 September 2017

Please cite this article as: F. Rodrigues, J. Pascoa, M. Trancossi, Heat Generation Mechanisms of DBD Plasma Actuators, *Experimental Thermal and Fluid Science* (2017), doi: http://dx.doi.org/10.1016/j.expthermflusci.2017.09.005

Heat Generation Mechanisms of DBD Plasma Actuators

Rodrigues, F.*, Pascoa, J.*

Centre for Mechanical and Aerospace Science and Technologies, FCT (Portuguese Foundation for Science and Technology) Research Unit No. 151, DEM, Universidade da Beira Interior, Covilha, Portugal

Trancossi, M.*

Material and Engineering Research Institute, ACES, Sheffield Hallam University, City Campus, Howard Street, Sheffield S1 1WB, UK

Abstract

During the last twenty years DBD plasma actuators have been known by their ability for boundary layer flow control applications. However, their usefulness is not limited to this application field, they also present great utility for applications within the field of heat transfer, such as a way to improve the aerodynamic efficiency of film cooling of gas turbine blades, or de-icing and ice formation prevention. Nevertheless, there is a relative lack of information about DBD's thermal characteristics and its heat generation mechanisms. This happens due to the extremely high electric fields in the plasma region and consequent impossibility of applying intrusive measurement techniques. Against this background, this work describes the physical mechanisms behind the generation of heat associated to the DBD plasma actuators operation. An experimental technique, based on calorimetric principles, was devised in order to quantify the heat energy generated during the plasma actuators operation. The influence of the dielectric thickness, as well as the dielectric material, were also evaluated during this work. The results were exposed and discussed with the purpose of a better understanding of the heat generation mechanisms behind the operation of DBD plasma actuators.

Keywords: Heat Generation, Plasma Actuators, Dielectric Barrier Discharge, Thermal Characterization

1. Introduction

In recent years DBD plasma actuators have been a subject of interest for the worldwide scientific community [1–3]. Several studies have demonstrated the potential of these actuators in separation control [4], wake control [5, 6], aircraft noise reduction [7], modification of velocity fluctuations [8, 9], and boundary layer control [10–13]. These devices have very attractive features including a very low mass, low power consumption, fast response time, being fully electronic and not presenting moving mechanical parts. Nowadays, they can even be simulated with different numerical solvers [14–20]. DBD plasma actuators are constituted by two electrodes separated by a dielectric layer (Figure 1). One of the electrodes is covered by the dielectric layer and is completely insulated from the other one, that is exposed to the air in the top of the dielectric. Thus, the electrodes are, respectively, designated as the covered electrode and the exposed electrode [21–23]. To operate a DBD plasma actuator the two electrodes should be connected to an AC high voltage and high frequency

*Corresponding author
Email address: frederic@ubi.pt (Rodrigues, F.)

power supply. When the amplitude of the voltage applied to the exposed electrode is large enough, ionization of the air (plasma) occurs over the surface of the dielectric, which in the presence of the electric field gradient produces a body force on the ambient air. Thus, the actuator induces a flow that draws air towards the surface of the actuator, and it accelerates this air downstream in a direction tangential to the dielectric [24–27].

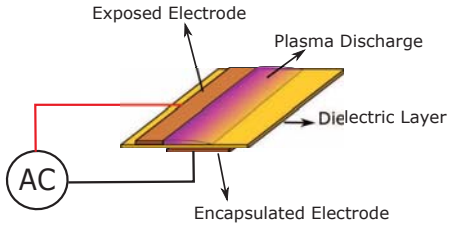

Figure 1: Schematic of Dielectric Barrier Discharge configuration.

Although the main applications of DBD plasma actuators are related to the field of flow control, these devices have also possible applications in the field of heat transfer, such as film cooling of turbine blades and heat generation for de-icing, or ice formation prevention. Some studies have already been conducted showing film cooling enhancement obtained by the operation of plasma actuators. Roy and Wang [28] numerically tested a plasma actuator for film cooling enhancement on a flat plate, while Yu et al. [29] studied film cooling performance for a cylindrical hole with plasma aerodynamic actuation. These studies demonstrated that plasma actuators allow to improve the film cooling effectiveness. However, the heat dissipated during the plasma actuators operation affects negatively the film cooling performance. To improve the plasma actuators performance, in film cooling applications, it is strictly necessary to understand the heat generation mechanisms behind their operation. Later the heat generation can be reduced in order to optimize the film cooling effectiveness. Regarding de-icing, or anti-icing applications, two recent studies were performed. In the work conducted by Meng et al. [30], the effects of plasma actuation on de-icing and anti-icing were studied by surface temperature measurements in quiescent air and icing wind tunnel, whereas in the study of Van den Broecke [31], nano second DBD plasma actuators were used for de-icing purposes. Both studies showed that plasma actuators are effective in de-icing and anti-icing applications. Conversely to film cooling applications, for de-icing and anti-icing purposes the objective is to increase the heat generated during the plasma actuators operation and, consequently, optimize the de-icing process. For this purpose it is first necessary to understand the heat generation mechanisms present in the plasma actuation.

Despite of the importance of plasma actuators for applications within the heat transfer field currently the thermal characteristics of DBDs are not completely known, as a result of the complex nature of plasma formation, which makes difficult the measurement of the various parameters involved. According to Tirumala et al. [32] due to the extremely high electric fields in the plasma region, and the impossibility of applying intrusive measurement techniques, the two measurement techniques that can be used are infra-red thermography and emission spectroscopy. However, in the present paper, we will present an alternative integral experimental technique which makes possible to quantify the fraction of power dissipated as heat.

Still there have been studies carried out to better understand the thermal behaviour of DBD plasma actuators. Roth et al. [33] conducted a study where they presented data on the physics and phenomenology of plasma actuators. They explained that the power consumed by plasma actuators is composed of the power dissipated by the surface discharge and the thermal dielectric losses. They estimated the power losses in a plasma actuator considering that the power losses in the dielectric increase linearly with the voltage frequency and also with the square of the voltage amplitude. The principle used to determine the thermal power dissipated in the dielectric, presented in the Roth's study, will be also used in the present work. However, we will also verify that this thermal power is just a small portion of the total thermal power released during the actuators operation. Dong et al. [34] measured the influence of the frequency and applied voltage level on the dissipated

power. They used an empirical formula, similar to the formula used by Roth et al. [33], to estimate the dissipated power and the energy loss in the dielectric. Plasma temperatures were also evaluated using spectroscopy emission measurements. The electrical power was measured for two dielectrics, epoxy and Teflon, for different thicknesses of the dielectric, and under various operating conditions (applied voltages and frequencies). They found that most of the active power is injected in the plasma, however, a large part of the remaining active power is directly transferred into the dielectric panel. Stanfield et al. [35] also conducted spectroscopy measurements of a DBD actuator in order to obtain the rotational temperature of the gas above the grounded electrode. They observed that the rotational temperatures of the gas decreased in the induced flow direction and increased with increasing voltage. Jukes et al. [36] observed the temporal and spatial structure of the plasma actuator induced flow. They used thermal imagery to estimate the surface temperature of the dielectric sheet, during plasma operation, and deduced an analytical formula to estimate the plasma gas temperature. Later on, Joussot et al. [37] performed a study where they used the Jukess analytical formula and concluded that this formula is not accurate enough to estimate the plasma gas temperature. In Jussot's study [37] the authors used infra-red thermography to determine the temperature of the dielectric surface with the plasma on, and after switching off the discharge. They concluded that the average surface temperature increased linearly with the electrical power, as it increased with the frequency and with the square of the voltage amplitude. The work performed by Erfani et al. [38] focused on the effect of actuator surface temperature and its aerodynamic performance. They conducted experiments with DBD plasma actuators applied in a surface at different temperatures (ambient temperature, -40^0C and 120^0C). The authors found that in a hotter actuator surface its possible to achieve higher velocities and higher body forces by consuming a slightly higher power. Tirumala et al. [32] also conducted infra-red thermography measurements on the surface of a thick, dielectric based, DBD actuator and characterized it against various electrical and geometrical parameters. They studied the temperature distribution and proposed an hypothesis on the mechanism of dielectric heating and a relationship between dielectric surface temperature and gas temperature. Aberoumand et al. [39] numerically studied the impact of different arrangements of dielectric barrier discharge plasma actuators on temperature field in a channel flow. The actuators were tested under an incompressible flow regime with a constant entrance Reynolds number. The authors verified the importance of heat generated by DBD plasma actuators operation and concluded that plasma actuators can be considered as beneficial instruments for increasing the temperature of the fluid. Furthermore, the authors have evidenced that the increase in temperature can be considerable and noted for related applications.

Recently Benmoussa et al. [40] conducted numerical investigations of the gas heating phenomenon in dielectric barrier discharges due to the joule heating effect for Ne-Xe gas mixtures. They observed that the gas temperature, close to the vicinity of the actuator, increase due to the high values of the power deposited in this region. They tested two different waveform shapes and showed that the gas temperature in DBD excited with rectangular applied voltage waveform reached higher values than with the discharge created by a sinusoidal excitation. Rodrigues et al. [41] conducted surface temperature measurements on actuators with different dielectric thicknesses and different dielectric materials under quiescent conditions. They verified that the temperature distribution is similar for the different test cases however the temperature levels change with the dielectric thickness and also with the type of dielectric material.

Further information can be found in the reviews of Bernard and Moreau [24] and Kotsonis [42] which compile the most relevant findings about DBD plasma actuators.

The present work aims to explain the heat generation mechanisms of DBD plasma actuators and quantify the heat generated by the plasma actuation. The total power consumed and the fraction of the consumed power dissipated as heat energy are some of the parameters with great interest in any heat transfer application of DBD plasma actuators [32]. So, in the present work, these parameters are herein ob-

tained by experimental measurements and discussed. An innovative experimental approach to quantify the thermal power generated by DBD plasma actuators is also described and justified. We found results for different dielectric layer materials and thicknesses. As we saw during the literature review presented above, the studies conducted about thermal characteristics of plasma actuators are focused on the dielectric temperatures distribution. The present study is focused on the quantification of energy, which is released in a form of heat providing a deep explanation about the heat generation mechanisms of DBD plasma actuators.

2. Experimental Setup and Procedure

An experimental setup was developed in order to operate the DBD plasma actuators and determine the heat generated during their actuation. The electrodes of DBD plasma actuators were made of copper tape and were asymmetrically mounted on either side of the dielectric, with no gap between them. The dimensions of the exposed electrode were $10mm$ width, $80mm$ length and $80\mu m$ thickness. The covered electrode had the same length and thickness of the exposed electrode, and $20mm$ width. The covered electrode was encapsulated with a thin Kapton layer which was also used to hold the wire to the covered electrode. In the present study we tested actuators with dielectric layer made of Kapton with different dielectric thicknesses and also actuators made of Polyisobutylene rubber, Polylactic Acid (PLA) and Acrylic Silicon, with same dielectric thickness of $1mm$. Plasma actuators were supplied by a high voltage and high frequency power supply, model PVM 500, manufactured by Information Unlimited, Inc. This power supply can produce voltages up to $20kV$ AC peak-to-peak with a frequency from $20kHz$ to $50kHz$ and at a current of $10mA$, so that the power ranges up to $200W$.

2.1. Electrical Characterization

For power consumption analysis, the voltage waveform was measured by a PicoScope model $5443A$. The PicoScope is an equipment that turns a normal computer into an oscilloscope. It is usually used in automotive diagnostics for fault-detection in sensors, actuators and electronic circuits. It allows the measurement of high voltage and current waveforms present in the system. Along with the PicoScope, a probe named Secondary Ignition Pickup allowed to measure the voltage and the frequency of the signal. This tool allows to make the measurements without cutting, disconnecting, or stripping out the wire. In order to obtain the current waveform a metal film resistor was placed in series with the plasma actuator. The resistor was connected between the covered electrode and the ground of the power source. The current trough the resistor was obtained from the voltage U_r measured across the resistor, by using Ohms law ($I_r = U_r/R$). Applying this method the voltage across the resistor is low enough to be measured by conventional instruments. Since the actuator was connected in series with the resistor the current trough the actuator is equal to the current trough the resistor ($I_a = I_r$). The metal film resistor used in the experiments has 100Ω of impedance with 1% of tolerance. Therefore, the impedance of the resistor is relatively low compared with the impedance of the actuator, not affecting its operation. This type of resistor was chosen because its impedance remains constant, even under temperature variations. The resistor used here has a temperature coefficient of $50ppm$, which means that the resistor impedance only varies $0.00005\Omega/^{O}C$. Therefore, this variation can be neglected in the power consumption analysis. The voltage and current waveforms are recorded and the instantaneous power is computed via point-by-point multiplication of the voltage and current data values, as described in,

$$P_a(t) = U(t).I(t). \tag{1}$$

Where $U(t)$ is the input voltage of the actuator, $I(t)$ is the current and $P(t)$ is the instantaneous power. By this way, the average power of n periods (T) is obtained by,

$$\bar{P}_a = \frac{1}{nT}\int_0^{nT} U(t).I(t)dt. \tag{2}$$

To fulfil the plasma actuator electrical characterization, Lissajous figures were drawn and fully inter-

preted. In order to represent the Lissajous figures a capacitor, with known capacitance, was placed in series between the covered electrode and the ground. The capacitor used was an $E222M$ which has $2,2nF$ of capacitance, 20% of tolerance and a rated voltage of $2kV$. The capacitor was chosen with a large value of Cm comparatively to the capacitance of the actuator without plasma discharge. By this way, the voltage drop across the capacitor is adequately low to be measured by conventional instruments. The instantaneous charge of the capacitor is given by,

$$Q_m(t) = C_m U_m(t). \tag{3}$$

Where Cm is the capacitor capacitance and Um is the voltage across the capacitor. The current trough the capacitor is given by,

$$I_m(t) = C_m \frac{\partial U_m(t)}{\partial t}. \tag{4}$$

Once the capacitor is connected in series with the actuator, we know that the current trough the capacitor is equal to the current trough the actuator ($Im = Ia$). So, the instantaneous power dissipated by the actuator can be obtained by equation,

$$P_a(t) = U_a(t).I_a(t) = U_a(t).C_m \frac{\partial U_m(t)}{\partial t}. \tag{5}$$

Where Ua is the voltage across the actuator and Ia is the current trough the actuator. The average power over n periods T is given by,

$$\bar{P}_a(t) = \frac{1}{nT} \int_0^{nT} U_a(t).C_m \frac{\partial U_m(t)}{\partial t} dt. \tag{6}$$

For one cycle we have,

$$\bar{P}_a(t) = \frac{1}{T} \int \int U_a \partial Q. \tag{7}$$

By eq. 7, we have that the instantaneous capacitor charge and the instantaneous actuator voltage, plotted against each other, generate a Lissajous curve, and the area inside the closed Lissajous curve divided by the period gives the actuator power consumption.

2.2. Quantification of the Generated Heat

In order to quantify the heat released by plasma actuators to the surrounding air, an experimental technique based on calorimetric principles was devised. In this technique the heat released by the plasma actuators was quantified by using a device, developed in the present work, which consists in a pipe with a fan at the inlet to provide a constant air flow (figure 2).

The actuator is placed inside the pipe through a lateral opening which is closed during the experiments. The pipe is coated by a layer of high quality cork with $3mm$ thickness which has a very low thermal conductivity ($\kappa = 0.04W/mK$) and prevent possible heat dissipation trough the wall of the pipe. The pipe used in this experiment presents a diameter of $4.3cm$ and a length of $21cm$. The inlet of the pipe contains a "Sunon" fan, model:$ME40101V1 - 000U - A99$ with dimensions $40 \times 40 \times 10mm$, which works at 12 Volt DC and produces a constant air flow of $13.6m^3/h$. Thus we have an air flow velocity of $2.6m/s$ (this velocity was confirmed by anemometer measurements) and the Reynolds number of the air flow is 7397 which means that we are quantifying the heat transfer in turbulent conditions. In our experiments these conditions are essential because they provide a higher heat transfer coefficient allowing a faster heat transfer process. During the experiment the temperature of the air flow is recorded at the outlet (at a $6cm$ distance from the plasma actuator) by means of a thermocouple, K type, with $2m$ cable length, a temperature range of -40^0C to 1200^0C, and a time response of $0.1s$. The thermocouple is connected to a thermo-booster pack coupled to a microcontroller TI Launchpad model MSP EXP430G2. The microcontroller is connected to the computer which makes the data acquisition of the thermocouples trough MatLab software.

To perform the experiments, the fan is turned on before the actuator operation and a stabilization time of $10s$ is considered to ensure the stabilization of the air flow temperature. Then the temperature is recorded during $30s$ (initial temperature) and after that the plasma actuator is ignited. The air flow temperature at the outlet is continuously monitored and as soon as it stabilizes it is recorded during $30s$ (final

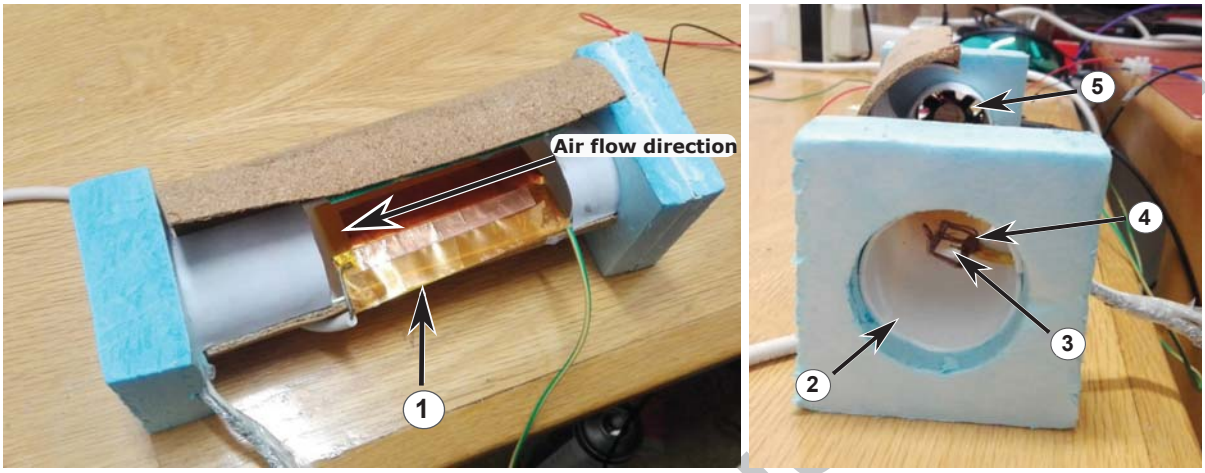

(a) Top view (b) Front view

Figure 2: Air flow calorimeter for quantification of heat generated by DBD plasma actuators. 1- DBD plasma actuator, 2- Air flow outlet, 3- Thermocouple, 4- Copper cage grounded to eliminate electromagnetic interference 5- Fan at the inlet which provides the air flow.

temperature). Considering the fundamental calorimetric law we know that, for an isobaric process, the heat energy transferred to a body is given by the equation:

$$Q = m.C_p.\Delta T. \tag{8}$$

Where m is the body mass, C_p is the specific heat at constant pressure, and ΔT is the temperature variation. In our specific case, the thermal energy released by the actuator will be transferred to the air flow. So, applying the fundamental calorimetric law, and substituting the mass by the mass flow rate ($\dot{m}$), we obtain the calorific energy transferred per second which actually is the thermal power dissipated by the actuator. The mass flow rate of air can be obtained by the density and air flow rate ($\dot{m} = \rho_{air}.\phi$) therefore the thermal power is given by,

$$P_T = \rho_{air}.\phi.C_p.\Delta T. \tag{9}$$

2.3. Electromagnetic Interference Mitigation

The extremely high electric field in the plasma region interferes with the thermocouples disabling the measurement of the temperature. This issue was solved making possible the temperature measurements. The thermocouple cables were completely shielded with aluminium foil which was grounded. The thermocouple hot junction was also shielded with a special small box made of copper sheet, without the frontal and back sides allowing the passage of the air flow trough it and making sure that the temperature measured by the thermocouple is equal to the temperature in the surrounding area. The microcontroller was also placed in a box shielded by aluminium foil and this box was placed at about $1.5m$ of distance from the actuator. This distance was found to be the necessary distance to avoid electromagnetic interference in the microcontroller operation. In addition, the signal measured by the thermocouple was filtered by means of a low-pass filter with a cut-off frequency in the order of $20kHz$.

2.4. Verification of the Experimental Method Accuracy

Before using this technique for heat generation quantification in plasma actuators we performed a

verification in order to ensure that the results obtained by this experimental method are accurate. This verification was made using an electric heater with $10cm$ length. The heater was placed inside the air flow calorimeter (in the same position that the plasma actuators where posteriorly tested) and the thermal power generated by the heater was quantified by using the calorimetric method. Since in a heater the input power is completely dissipated by Joule effect, the input power was measured and correlated with the results obtained by the calorimetric experiments. This validation was made for different voltage levels and the obtained results are presented in figure 3

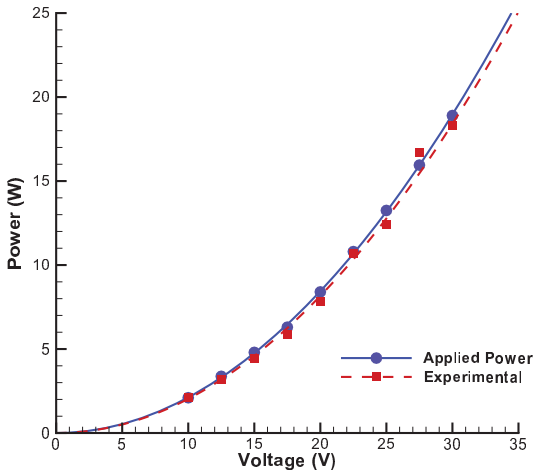

Figure 3: Validation of the experimental method.

The experimental results presented in the graph were obtained by averaging 5 tests at same applied voltage. We verified that if we perform only one experiment the obtained results are not accurate, but by averaging 5 experiments at same applied voltage the error associated to this experimental procedure is reduced. By this way the relative error associated to the experiment is less than 10% which indicates a good accuracy of the results.

3. Results and Discussion

During this work we realised that heat generation in DBD plasma actuators is largely influenced by the characteristics of the dielectric layer. Then, in the following results, we explain the influence of the dielectric material and thickness. First we present an electrical characterization of the different actuators tested. Later we quantify the thermal power generated by different plasma actuators operating at different voltage levels and then we provide a physical explanation, based on the experimental results otained, about the heat generation mechanisms in DBD plasma actuators.

3.1. Electrical Characterization

The power consumption of DBD plasma actuators was computed by using the electric current method. The voltage and current waveforms were recorded and power consumption was obtained by equation 2. To obtain more accurate results the power consumption was computed over 12 ac voltage cycles. Figure 4 shows typical current and voltage waveforms of a DBD plasma actuator. The current and voltage waveforms were acquired with a sampling rate of $125MS/s$ and a vertical resolution of 14 bits.

The voltage and current waveforms present a sinusoidal shape, however, the current waveform contains a series of high-amplitude spikes. These spikes are the result of each micro-discharge that leads to a fast electrical impedance change within the actuator. Therefore, we can observe current spikes two times per each current cycle, at the same time that occurs the plasma discharge. As expected, the current and voltage signals are approximately 90^0 out of phase, with the current leading the voltage.

The electric charge method was applied in order to compute the charge of the plasma actuator. Plotting the charge against the applied voltage we obtain the Lissajous curves.

Figure 5 shows the experimental Lissajous curves obtained for a DBD plasma actuator at different input voltages.

The Lissajous figures show the evolution of the actuator charge during the AC voltage cycle. As shown in figure 5 the analysis of these cyclograms provides

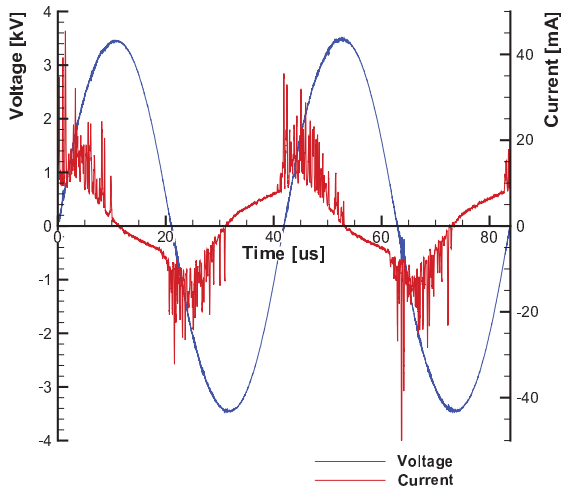

Figure 4: Typical voltage and current waveforms of a DBD plasma actuator (acquired for a $0.6mm$ kapton actuator at $7kVpp$ and $24kHz$).

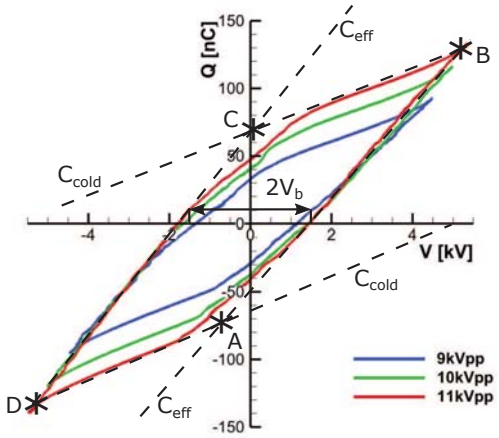

Figure 5: Experimental Lissajous figures obtained for a DBD plasma actuator with a dielectric layer of $0.84mm$ Kapton at $24kHz$.

important features about the DBD plasma actuator. The Lissajous figures reveal a parallelogram which is defined in figure 5 by the points ABCD. As explained in Mei et al.[43] the line segments BC and DA correspond to the discharge-off phase and their slopes provide the cold capacitance C_{cold} of the actuator. On the other hand the line segments AB and CD correspond to the discharge-on, so then the slopes of these lines provide the actuator effective capacitance C_{eff}. The distance between the two points in which the parallelogram intersects the x-axis is equal to twice the breakdown voltage. These parameters obtained by the analysis of the Lissajous curves are compiled in the table 1

Table 1: Parameters extracted from Lissajous curves.

Dielectric	$Vbd\ [kVpp]$	$C_{eff}\ [pF]$	$C_{cold}\ [pF]$
Kapton $0.30mm$	2.92	47.09	11.98
Kapton $0.60mm$	3.04	43.97	10.61
Kapton $0.84mm$	3.15	33.82	11.98
Kapton $1.02mm$	3.26	31.61	12.01
PIB Rub. $1mm$	3.43	26.57	3.79
PLA $1mm$	3.36	29.80	9.99
Silicone $1mm$	2.74	25.37	13.58

Looking to the parameters presented in table 1, we see that plasma actuator capacitances are lower for actuators with thicker dielectrics. This is in accordance with the typical behaviour of a capacitor whose capacitance decreases when the distance between the electrodes is increased. As expected the breakdown voltage increase with the increasing of the dielectric thickness, depending also on the dielectric material used.

3.2. Physical Mechanisms and Heat Generation Quantification

During the present work we were able to understand that the total heat released during the plasma

actuators operation is generated by two main mechanisms based on dielectric heating and gas heating. The total heat generated was quantified by the experimental procedure explained previously in section 2.2. A parcel of the total thermal power results from the power losses in the dielectric. Following Kraus [44] and Roth et al. [33] the parcel of thermal power originated in the dielectric can be obtained by:

$$P_D = U^2 \frac{2\pi f A}{d} \epsilon_R \epsilon_0 tan(\delta) \qquad [W]. \qquad (10)$$

Where U is the voltage f is the frequency, A is the area, d is the distance between the electrodes, ϵ_R is the relative permittivity of dielectric, ϵ_0 is the permittivity of vacuum and $tan(\delta)$ is the dielectric loss tangent or dissipation factor. This analytical method implies that the material used in the dielectric layer is a good insulator, with a low dissipation factor.

3.2.1. Heat Generation Without Plasma Formation

In a first approach, we studied the DBD plasma actuators operation without plasma discharge. For that purpose, the actuators were analysed operating at a range of voltages between $1kVpp$ and $3.5kVpp$. This range was considered because it includes the voltage levels which are not high enough to generate plasma, and the minimum voltage levels needed to ignite the plasma discharge. The active power applied to the plasma actuators was measured and the power dissipated in dielectric heating was estimated trough equation 10. For Kapton it was considered the tabulated values for dielectric permittivity of 3.5 and tangent loss of 0.002 [45]. Besides Kapton, three different dielectric materials were studied: Polylactic Acid (PLA), Poly-Isobutilene (PIB) Rubber and Acetoxy Silicone. The tabulated values of these materials considered for dielectric thermal power estimation were: Polylactic Acid, dielectric permittivity of 3.2 and tangent loss of 0.0035 [46]; Poly-Isobutylene Rubber, dielectric permittivity of 2.82 and tangent loss of 0.0015 (following fabricator informations); Acetoxy Silicone, dielectric permittivity of 3.6 and tangent loss of 0.0021 [47]. Figure 6 shows the results obtained for actuators made of Kapton with different dielectric thicknesses and actuators made of PLA, PIB rubber and Silicone with $1mm$ thickness. These results were obtained for an applied frequency of $24kHz$ and the uncertainty of the active power measurement is about 1%.

In figure 6 we see that for lower input voltages (up to $2kVpp$) the active power is almost equal to the thermal power dissipated in the dielectric. This happens because, at these voltage levels, there is no plasma formation and the actuator does not transfer momentum to the surrounding air. So the active power applied to the actuator is completely converted in dielectric heating. For voltages closer to the breakdown voltage the active power departs from the power dissipated in dielectric. This indicates that although the plasma is still not visible, the ignition of the discharge is starting. The ionization of the air starts and therefore a portion of the consumed power is spent in gas heating and electron collisions, while the other portion is transferred to the adjacent air, accelerating it. This phenomena is observed in figure 6 for any actuator tested. However, depending on the thickness and type of dielectric material, the ignition of the plasma occurs at different input voltages. Notice that the actuator with a dielectric layer made of $0.3mm$ kapton present a faster exponential evolution than the remaining actuators. As we saw in the electrical characterization section, plasma actuators with thin dielectric layers present lower breakdown voltage than actuators with thick dielectric layers. Thus, in thin actuators the discharge ignites for lower voltage levels and therefore they present a faster exponential growth than actuators with thicker dielectrics. In the case of the PLA actuator, even for an applied voltage of $3.5kVpp$ the input power is still completely consumed in dielectric. The active power only becomes higher than the power dissipated in dielectric for voltages higher than $3.5kVpp$. This happens because it has a dielectric dissipation factor higher than the other tested materials so, the portion of heat generated in dielectric is more significant than in the remaining actuators. An opposite behaviour was observed in the PIB Rubber actuator, which has a lower dielectric dissipation factor and therefore the active power departs from the thermal dielectric power for voltages higher than $1.5kVpp$.

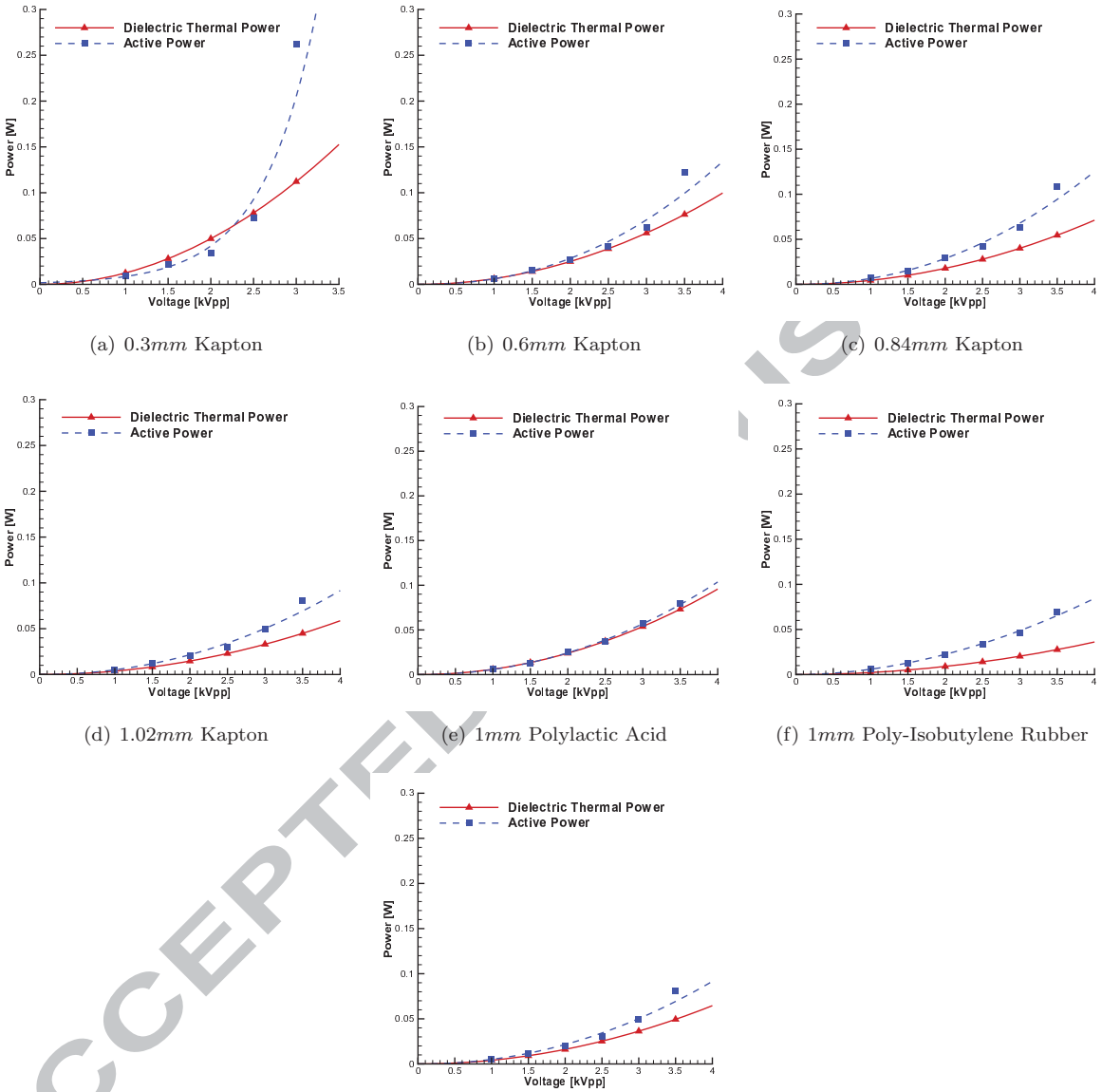

(a) 0.3mm Kapton (b) 0.6mm Kapton (c) 0.84mm Kapton

(d) 1.02mm Kapton (e) 1mm Polylactic Acid (f) 1mm Poly-Isobutylene Rubber

(g) 1mm Acetoxy Silicone

Figure 6: Active power versus power dissipated in dielectric heating for different thicknesses.

3.2.2. Total Heat Generation Quantification

In a second approach, DBD plasma actuators were studied at voltages above the breakdown voltage. In this operation regime there is plasma formation so then, the total heat released by the actuator is provided from dielectric heating and gas heating. The

total thermal power generated by the actuator was obtained experimentally trough the air flow calorimetric technique. Figure 7 shows the results obtained for actuators made of Kapton with different dielectric thicknesses, at the same frequency of $24kHz$.

From analysis of figure 7 we realised that the thermal power originated in dielectric represents just a small portion of the total thermal power released during the plasma actuator operation. The actuators with thicker dielectrics ($0.6mm$, $0.84mm$ and $1.02mm$ of thickness) show a similar behaviour between them in terms of thermal power released. The power converted in dielectric heating represents less than 10% of the active power and this percentage decreases with the growth of the input voltage. The majority of the thermal power released by the actuator comes from the gas heating being about 70% to 85% of the active power. The actuator with the thinnest dielectric ($0.3mm$ thickness) presents a slightly different behaviour. Similarly to the remaining Kapton actuators the power consumed in dielectric heating is less than 10% of the active power and this percentage decreases with the growth of the input voltage. But, in terms of the gas heating generated during the operation, we verified that it varies between 40% to 65% of the active power. Since the dielectric heating represents less than 10% of the active power, the thermal power generated by gas heating has a direct influence on the total thermal power behaviour. Then, in the actuator with thinnest dielectric ($0.3mm$ thickness) 45% to 70% of the active power is released in the form of heat, and in the remaining test cases ($0.6mm$, $0.84mm$ and $1.02mm$ thickness) the percentage of active power converted in heat is even higher, being 75% to 95% of the active power. Although the thinnest actuator presents a lower percentage of active power converted in heat, it presents high values of thermal power released to the adjacent airflow (for the same applied voltage). This is in accordance with the results presented in Rodrigues et al. [41], where the authors verified that, at the same applied voltage, the temperature levels are higher for thin dielectrics.

We verified that the percentage of active power converted in heat is lower in actuators with thin dielectrics therefore, we deduce that the percentage of power used to accelerate the adjacent flow in actuators with thin dielectrics is higher than in actuators with thick dielectrics. This evidence is in accordance with the works of Thomas et al. [48], Dong et al. [34] and Forte et al., [49] in which the authors verified, by velocity measurements, that the induced velocity at same applied voltage is higher in actuators with thin dielectrics.

The total thermal power generated in plasma actuators with different dielectric materials was also studied. Figure 8 presents the results obtained for actuators made of Polylactic Acid, Poly-Isobutylene Rubber and Acetoxy Silicone with same dielectric thickness ($1mm$) and operating at a frequency of $24kHz$. Regarding the power generated by dielectric heating the behaviour of the actuators tested with different dielectric materials is very similar to the behaviour of Kapton actuators. The power converted in dielectric heating represents just a small percentage of the active power and this percentage decreases with the growth of the input voltage. In the actuators made of Silicone and PIB rubber the dielectric heating is less than 10% of the active power and in the PLA actuator it is less than 12% of the active power. In terms of total thermal power generated, the PLA actuator and the Silicon actuator present a production of heat similar to the $1.02mm$ Kapton actuator, being that 75% to 95% of the active power is converted in heat. However, at same input voltages, the Silicon actuator presents lower consumed power and therefore lower values of total thermal power. The PIB rubber actuator was found to be the actuator with lower thermal power production which makes sense because, considering the tested materials, it has the lowest dielectric dissipation factor. From the analysis of figure 8 we verified that the total thermal power released by the PIB rubber actuator varies between 50% to 60% of the active power.

As we see in table 2, in general, plasma actuators present a good ability for heat production. In terms of thickness, we found that the use of thin dielectrics reduces the heat generation efficiency of plasma actuators, while the use of thicker dielectrics allow to achieve high heat production efficiencies. The dielectric layer material also present an important role on the heat generation efficiency. For actuators with $1mm$ of dielectric thickness we found that Kapton,

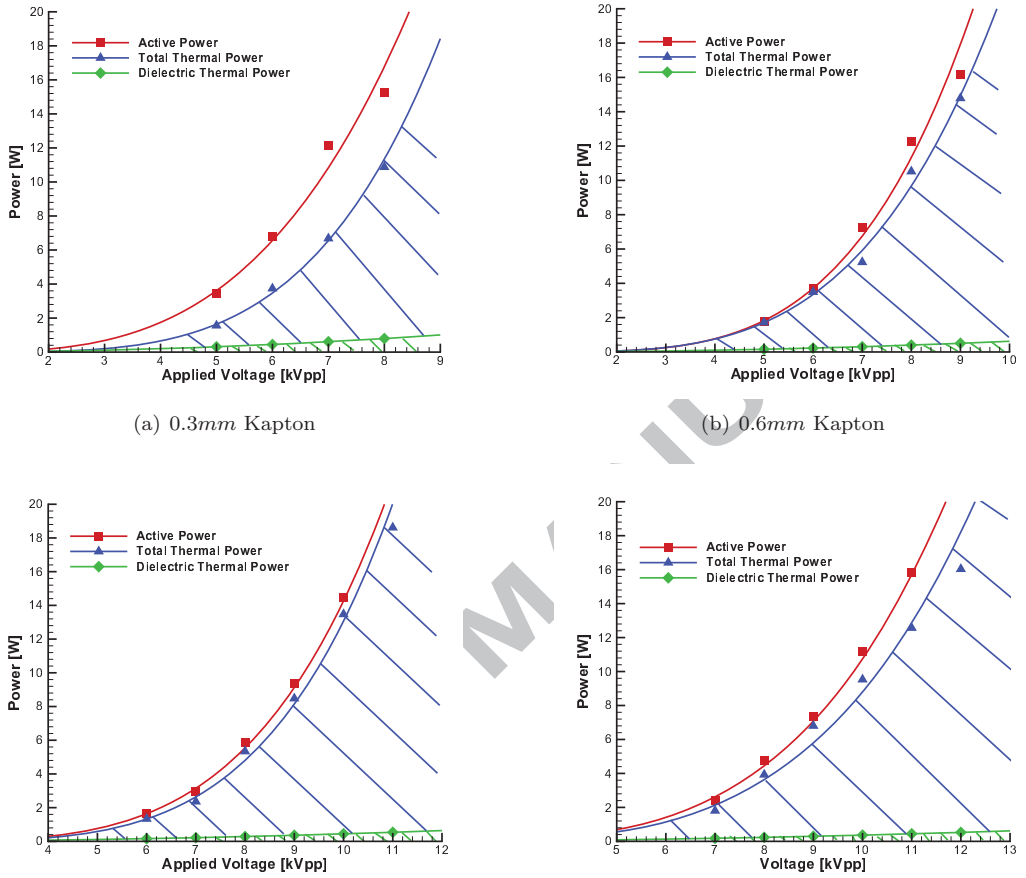

(a) 0.3mm Kapton

(b) 0.6mm Kapton

(c) 0.84mm Kapton

(d) 1.02mm Kapton

Figure 7: Active power versus thermal power.

PLA and Silicon are dielectrics which confers to the actuator high heat generation efficiencies. The average heat generation efficiencies founded for thick actuators made of these dielectrics (Kapton, PLA and Silicon) are comprised in a range of $80\% - 90\%$. In contrast, we found that the use of PIB rubber, as dielectric layer, implies a reduction on the heat generation efficiency of the plasma actuator, presenting an average heat generation efficiency of about 50%.

In the present study we verified that the type of dielectric material has a direct influence on the heat generation efficiency of the plasma actuator. The results indicate that the use of dielectrics with low dielectric permittivity, such as PIB rubber ($\epsilon = 2.82$), leads to a lower heat generation efficiency while dielectric materials with higher dielectric permittivity, such as Kapton ($\epsilon = 3.5$), PLA ($\epsilon = 3.2$) and Silicon ($\epsilon = 3.6$), lead to a higher heat generation efficiency. Our results also showed that the dielectric dissipation factor has a great influence on the heat dissipated by dielectric hysteresis phenomenon, but its impact is not reflected on the total thermal power, because al-

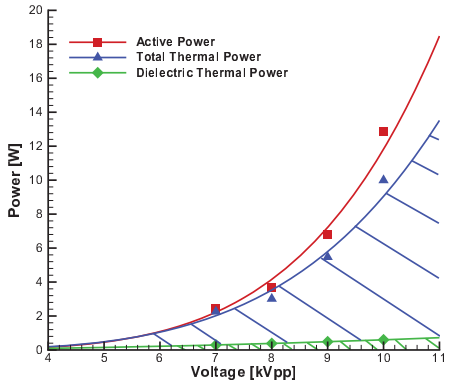

(a) Polylactic Acid

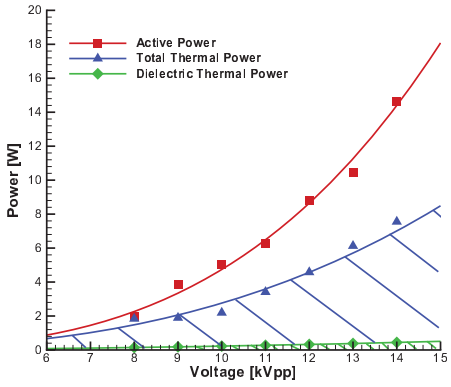

(b) Poly-Isubotylene Rubber

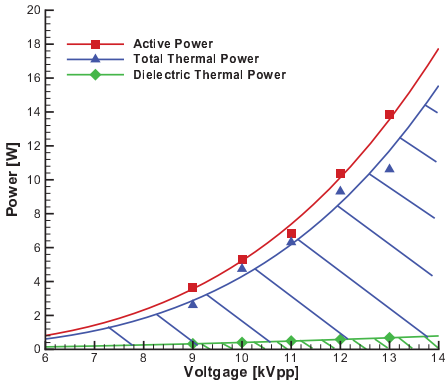

(c) Acetoxy Silicone

Figure 8: Active power versus thermal power.

though Kapton, PLA and Silicon have different dissipation factors (Kapton dissipation factor= 0.002; PLA dissipation factor= 0.0035; Silicon dissipation factor= 0.0021) the average heat generation efficiency obtained for them was very similar. Thus we may conclude that the dielectric permittivity of the material has a significant impact on the heat generation efficiency of plasma actuators while the dissipation factor influence is not reflected on the total thermal power produced.

Considering the possible applications of DBD plasma actuators in the field of heat transfer, we concluded that actuators with thin dielectric layers are the best option for applications in which the generation of heat is undesirable, such as film cooling applications. On the other hand, in de-icing and anti-icing applications the heat generated by plasma actuators is essential and therefore thick dielectrics may be used because they present higher heat generation efficiencies. The dielectric material of the plasma actuator has also a significant influence on the heat generation efficiency. We verified that actuators made

Table 2: Average heat generation efficiency.

Dielectric	Average Efficiency (η)
Kapton $0.30mm$	57%
Kapton $0.60mm$	88%
Kapton $0.84mm$	88%
Kapton $1.02mm$	83%
PIB Rubber $1mm$	52%
PLA $1mm$	83%
Silicone $1mm$	84%

of dielectrics as PLA, Kapton and Silicon are suitable for de-icing and anti-icing applications once they favour the heat generation during the plasma operation. Conversely, the PIB rubber actuator presents the desirable behaviour for film cooling applications, since during its operation just about 50% of the active power is converted in thermal power.

As explained in section 2.2 we are quantifying the heat transfer in turbulent conditions. As explained in the study of Joussot et al. [37] the external flow presents an important role on the dielectric surface temperature. The external flow increases the heat transfer coefficient and therefore the dielectric surface temperature will be lower than in quiescent conditions. By the same way, in turbulence conditions the air flow velocities are higher, so the dielectric surface temperature will be lower than in laminar conditions. The thermal power transferred to the external flow will present an inverse behaviour of the surface temperature, because when we increase the velocity of the external flow we increase the heat transfer between the actuator and the external flow. So, in theory the thermal power dissipated to the flow describes an inverse behaviour to the dielectric surface temperature and experiments in laminar flow conditions would provide us lower thermal power rates.

3.2.3. Heat Generation Mechanisms in DBD Plasma Actuators

During the present work we understood that there are two main mechanisms responsible for heat generation in DBD's: the dielectric heat generation mechanism and the gas heat generation mechanism. The dielectric heating occurs due to the dielectric hysteresis phenomenon. In dielectrics, considered good insulators, the DC conduction current can be negligible. Yet, an appreciable AC current, in phase with the applied field must be considered due to the dielectric hysteresis. The dielectric hysteresis is a similar phenomenon to the hysteresis found in ferromagnetic materials. Due to this effect dielectric materials may consume considerable energy in alternating fields, which is lost in a form of heat.

When the input voltage of DBD actuators is not high enough to originate plasma discharge, the power consumed by the actuators is completely converted in dielectric heating due to this phenomenon. When there is plasma discharge the dielectric heating is just a parcel of the total thermal power released by the actuator. Increasing the input voltage the dielectric heating phenomenon loses it significance and the percentage of thermal power generated in the dielectric decreases. When the actuator operates at voltages above the breakdown voltage, the main mechanism of heat generation is the gas heating. The gas heating is originated by electron elastic collisions, rotational and vibrational excitation, ion-neutral molecule collisions and thermal energy transferred from electrons to neutral particles. The gas heating is responsible by the major parcel of thermal power generated by DBD actuators, representing more than 85% of the total thermal power.

4. Conclusions

In the present work the thermal behaviour of different plasma actuators was studied with emphasis on the influence of the dielectric thickness and dielectric material. An air flow calorimetric technique was presented and explained, and its ability for thermal power quantification was demonstrated. The heat released by DBD actuators operation is provided by two main sources: dielectric heating and gas

heating. The heat in dielectric is originated due to the dielectric hysteresis phenomenon which leads to the consumption of considerable energy in a form of heat. The gas heating is originated by electron elastic collisions, rotational and vibrational excitation, ion-neutral molecule collisions and thermal energy transferred from electrons to neutral particles. The experimental results showed that when the actuator operates at voltages lower than the breakdown voltage, the power consumed by the actuator is completely converted in heat due to the dielectric hysteresis effect. When plasma actuators are operating above the breakdown voltage, the active power is converted in dielectric heating, gas heating and momentum which is transferred to the surrounding air. For voltages above the breakdown voltage, the gas heating is responsible for the majority of the thermal power produced by the actuator. The portion of thermal power originated from the dielectric heating is more significant for voltages near the breakdown voltage and it looses its significance when we increase the input voltage. We also verified that the type of dielectric material has a direct influence on the heat generation efficiency of the plasma actuator. We concluded that the dielectric permittivity of the material has a significant impact on the heat generation efficiency of plasma actuators while the dissipation factor influence is not reflected on the total thermal power produced.

The present study allowed to understand the physical mechanisms behind the plasma actuators operation providing important information for their application in the heat transfer field. From the analysis of actuators with different dielectric thicknesses we concluded that plasma actuators with thin dielectrics present a lower percentage of active power converted in heat, therefore they are suitable for applications in which the heat generation is undesirable. On the other hand, plasma actuators with thick dielectrics favour the heat generation during the plasma actuation thus, they are suitable for applications in which the heat generation is essential. We also verified that the choice of the dielectric material should be done considering the type of heat transfer application. From the different dielectric materials tested, we verified that PLA and Kapton actuators present a high thermal power generation, which makes them suitable for applications involving heat production. The PIB rubber actuator demonstrated to have an opposite behaviour. Only half of the active power is released in the form of heat which indicates that this actuator is appropriate for applications which require minimized heat production.

Acknowledgements

The present work was supported by European FP7 Project "ACHEON- Aerial Coanda High Efficiency Orienting-jet Nozzle", Grant No. 309041, part of the work was also supported by Portuguese Foundation for Science and Technology (FCT) with Grant No. SFRH/BD/110529/2015 trough the POCH program, and by FCT project PTDC/EMS-ENE/5742/2014 "Unsteady Boundary Layer Flow Control Using Plasma Actuators of Next Generation" trough the POCI program. Additional financial support was provided by C-MAST - Center for Mechanical and Aerospace Sciences and Technologies, Research Unit No. 151.

Nomenclature

ΔT	Temperature variation.
$\dot{m}$	Mass Flow Rate.
ϵ_0	Vacuum permittivity.
ϵ_R	Relative permittivity.
κ	Thermal conductivity.
ϕ	Air Flow Rate.
ρ	Density.
A	Area
C_p	Specific heat at constant pressure.
d	Dielectric thickness.
f	Frequency.
I_a	Current trough the actuator.

	I_r	Current trough the resistor.
	m	Mass.
	P_D	Power Converted in Dielectric Heating.
	P_T	Thermal Power.
	Q	Calorific energy.
	R	Resistance.
	U	Voltage.
	U_r	Voltage across the resistor.

References

[1] E. Pescini, M. Giorgi, L. Francioso, A. Sciolti, A. Ficarrella, Effect of a micro dielectric barrier discharge plasma actuator on quiescent flow, IET Science, Measurement and Technology 8 (2014) 135–142.

[2] T. C. Corke, C. L. Enloe, S. P. Wilkinson, Dielectric barrier discharge plasma actuators for flow control, Annual Reviews of Fluid Mechanics 42 (2010) 505–529.

[3] B. Jayaraman, S. Thakur, W. Shyy, Modeling of fluid dynamics and heat transfer induced by dielectric barrier plasma actuator, Journal of Heat Transfer 129 (2007) 517–525.

[4] C. L. Kelley, P. Bowles, J. Cooney, C. He, T. C. Corke, High mach number leading-edge flow separation control using ac dbd plasma actuators, in: 50th AIAA Aerospace Sciences Meeting Including the New Horizons Forum and Aerospace Exposition, AIAA 2012-0906, 2012, pp. 1–22.

[5] A. V. Kozlov, Plasma actuators for bluff body flow control, Ph.D. thesis, Graduate School of the University of Notre Dame, 2010.

[6] F. O. Thomas, A. Kozlov, T. C. Corke, Plasma actuators for cylinder flow control and noise reduction, AIAA Journal 46 (2008) 1921–1931.

[7] X. Huang, X. Zhang, Streamwise and spanwise plasma actuators for flow-induced cavity noise control, Physics of Fluids 20 (2008) 1–10.

[8] S. Grundmann, C. Tropea, Experimental damping of boundary-layer oscillations using dbd plasma actuators, International Journal of Heat and Fluid Flow 30 (2009) 394–402.

[9] S. Grundmann, C. Tropea, Active cancellation of artificially introduced tollmien-schlichting waves using plasma actuators, Experiments in Fluids 44 (2008) 795–806.

[10] E. Pescini, F. Marra, M. Giorgi, L. Francioso, A. Ficarrella, Investigation of the boundary layer characteristics for assessing the dbd plasma actuator control of the separated flow at low reynolds numbers, Experimental Thermal and Fluid Science 81 (2017) 482–498.

[11] M. Abdollahzadeh, F. Rodrigues, J. C. Pascoa, P. J. Oliveira, Numerical design and analysis of a multi-dbd actuator configuration for the experimental testing of acheon nozzle model, Aerospace Science and Technology 41 (2015) 259–273.

[12] R. Joussot, D. Hong, R. Weber-Rozenbaum, A. Leroy-Chesneau, Modification of the laminar-to-turbulent transition on a flat plate using a dbd plasma actuator, in: 5th Flow Control Conference, AIAA 2010-4708, 2010, pp. 1–8.

[13] S. Grundmann, C. Tropea, Experimental transition delay using glow-discharge plasma actuators, Experiments in Fluids 42 (2007) 653–657.

[14] M. Abdollahzadeh, J. C. Pascoa, P. J. Oliveira, Modified split-potential model for modeling the effect of dbd plasma actuators in high altitude flow control, Current Applied Physics 14 (2014) 1160–1170.

[15] M. Kotsonis, S. Ghaemi, L. Veldhuis, F. Scarano, Measurementof the body force field of plasma actuators, Journal of Physics D: Applied Physics 44 (2011) 11pp.

[16] T. C. Corke, M. L. Post, D. M. Orlov, Single dielectric barrier discharge plasma enhanced aerodynamics: physics, modeling and applications, Experiments in Fluids 46 (2009) 1–26.

[17] K. P. Singh, S. Roy, Force approximation for a plasma actuator operating in atmospheric air, Journal of Applied Physics 103 (2008) 1–6.

[18] K. P. Singh, S. Roy, Modling plasma actuators with air chemistry for effective flow control, Journal of Applied Physics 101 (2007) 1–8.

[19] J. R. Roth, X. Dai, Optimization of the aerodynamic plasma actuator as an electrohydrodynamic (ehd) electrical device, in: 44th AIAA Aerospace Sciences Meeting and Exhibit, AIAA 2006-1203, 2006, pp. 1–28.

[20] C. L. Enloe, T. E. McLaughlin, G. I. Font, J. W. Baughn, Parameterization of temporal structure in the single-dielectric-barrier aerodynamic plasma actuator, AIAA Journal 44 (2006) 1127–1136.

[21] R. Erfani, H. Zare-Behtash, C. Hale, K. Kontis, Development of dbd plasma actuators: The double encapsulated electrode, Acta Astronautica 109 (2015) 132–143.

[22] T. G. Nichols, J. L. Rovey, Surface potential and electric field measurements in plasma actuators at low pressure, AIAA Journal 51 (2013) 1054–1065.

[23] J. W. Ferry, Thrust measurement of dielectric barrier discharge plasma actuators and power requirements for aerodynamic control, Master's thesis, Missouri University of Science and Technology, 2010.

[24] N. Bernard, E. Moreau, Electrical and mechanical characteristics of surface ac dielectric barrier discharge plasma actuators applied to airflow control, Experiments in Fluids 55 (2014) 1–43.

[25] I. Maden, R. Maduta, J. Kriegseis, S. Jakirlic, C. Schwarz, S. Grundmann, C. Tropea, Experimental and computational study of the flow induced by a plasma actuator, International Journal of Heat and Fluid Flow 41 (2013) 80–89.

[26] L. N. Cattafesta, M. Sheplak, Actuators for active flow control, Annual Reviews of Fluid Mechanics 43 (2011) 247–272.

[27] G. I. Font, C. L. Enloe, T. E. McLaughlin, Plasma volumetric effects on the force production of a plasma actuator, AIAA Journal 48 (2010) 1869–1874.

[28] S. Roy, C. Wang, Numerical investigation of three-dimensional plasma actuation for improving film cooling effectiveness, Journal of Thermophysics and Heat Transfer 27 (2013) 489–497.

[29] J. Yu, L. He, W. Zhu, W. Ding, Y. Wang, Numerical simulation of the effect of plasma aerodynamic actuation on improving film hole cooling performance, Heat Mass Transfer 49 (2013) 897–906.

[30] X. Meng, J. Cai, Y. Tian, X. Han, D. Zhang, H. Hu, Experimental study of deicing and anticing on a cylinder by dbd plasma actuation, in: 47th AIAA Plasmadynamics and Lasers Conference, AIAA 2016-4019, 2016, pp. 1–14.

[31] J. Van den Broecke, De-icing using ns-DBD plasma actuators - Efficiency and de-icing capability of nanosecond pulsed dielectric barrier discharge plasma actuators, Master's thesis, Delft University of Technology, 2016.

[32] R. Tirumala, N. Bernard, E. Moreau, M. Fenot, G. Lalizel, E. Dorignac, Temperature characterization of dielectric barrier discharge actuators: influence of electrical and geometric parameters, Journal of Physics D: Applied Physics 47 (2014) 1–12.

[33] J. R. Roth, X. Dai, J. Rahel, D. M. Shermann, The physics and phenomenology of paraelectric one atmosphere uniform glow discharge plasma

(oaugdp) actuators for aerodynamic flow control, in: 43rd AIAA Aerospace Sciences Meeting and Exhibit, AIAA 2005-781, 2005, pp. 1–11.

[34] B. Dong, J. M. Bauchire, J. M. Pouvesle, P. Magnier, D. Hong, Experimental study of a dbd surface discharge for the active control of subsonic airflow, Journal of Physics D: Applied Physics 41 (2008) 1–9.

[35] S. A. Stanfield, J. Menart, C. DeJoseph, R. L. Kimmel, J. R. Hayes, Rotational and vibrational temperature distributions for a dielectric barrier discharge in air, AIAA Journal 47 (2009) 1107–1115.

[36] T. N. Jukes, K. Choi, T. Segawa, H. Yoshida, Jet flow induced by a surface plasma actuator, in: Proceedings of the Institution of Mechanical Engineers Part I: Journal of Systems and Control Engineering, volume 222, 2008, pp. 347–356. doi:10.1243/09596518JSCE504.

[37] R. Joussot, D. Hong, H. Rabat, V. Boucinha, R. Weber-Rozenbaum, A. Leroy-Chesneau, Thermal characterization of a dbd plasma actuator: Dielectric temperature measurements using infrared thermography, in: 40th Fluid Dynamics Conference and Exhibit, AIAA 2010-5102, 2010, pp. 1–8.

[38] R. Erfani, H. Zare-Behtash, K. Kontis, Plasma actuator: Influence of dielectric surface temperature, Experimental Thermal and Fluid Science 42 (2012) 258–264.

[39] A. Aberoumand, S.and Jafarimighaddam, T. Aberoumand, H.and Iran, Numerical investigation on the impact of dbd plasma actuators ontemperature enhancement in the channel flow, Heat Transfer - Asian Research 0 (2016) 1–14.

[40] A. Benmoussa, A. Belasri, Z. Harrache, Numerical investigation of gas heat effect in dielectric barrier discharge for ne-xe excilamp, Current Applied Physics 17 (2017) 479–483.

[41] F. Rodrigues, J. C. Pascoa, M. Trancossi, Experimental thermal characterization of dbd plasma actuators, in: ASME 2017 International Mechanical Engineering Congress & Exposition, 2017, pp. 1–12.

[42] M. Kotsonis, Diagnostics for characterisation of plasma actuators, Measurement Science and Technology 26 (2015) 30.

[43] D. Mei, X. Zhu, Y. He, J. D. Yan, X. Tu, Plasma-assisted conversion of co2 in a dielectric barrier discharge reactor: understanding the effect of packing materials, Plasma Sources Science and Technology 24 (2015) 10pp.

[44] J. Kraus, Electromagnetics, 4th ed., McGraw-Hill Inc., 1991.

[45] X. Wang, J. Engel, C. Liu, Liquid crystal polymer (lcp) for mems: processes and applications, Journal of Micromechanics and Microengineering 13 (2003) 628–633.

[46] S. Ebnesajjad, Handbook of Biopolymers and Biodegradable Plastics. Properties, Processing and Applications, Elsevier, 2013.

[47] H. Dodiuk, G. S. H. (Eds.), Handbook of Thermoset Plastics, Elsevier, 2014.

[48] F. O. Thomas, T. C. Corke, M. Iqbal, A. Kozlov, D. Schatzman, Optimization of dielectric barrier discharge plasma actuators for active aerodynamic flow control, AIAA Journal 47 (2009) 2169–2177.

[49] M. Forte, J. Jolibois, J. Pons, E. Moreau, G. Touchard, M. Cazalens, Optimization of a dielectric barrier discharge actuator by stationary and non-stationary measurements of the induced flow velocity; application to airflow control, Experiments in Fluids 43 (2007) 917–928.